A MICROFLUIDIC BIOSENSING ARCHITECTURE FOR MULTIPLEXED ANALYTE DETECTION USING HYDROGEL BARCODED PARTICLES

By

SHREYA PRAKASH

A thesis submitted to the

School of Graduate Studies

Rutgers, The State University of New Jersey

In partial fulfillment of the requirements

For the degree of

Master of Science

Graduate Program in Electrical and Computer Engineering

Written under the direction of

Dr. Umer Hassan

And approved by

_____

_____

_____

New Brunswick, New Jersey

October 2019

ABSTRACT OF THE THESIS

A MICROFLUIDIC BIOSENSING ARCHITECTURE FOR MULTIPLEXED ANALYTE DETECTION USING HYDROGEL BARCODED PARTICLES

by Shreya Prakash

Thesis Director: Dr. Umer Hassan

Multiplexing is a method of analyzing multiple analytes in a biological assay in a single step. It provides advantage of shorter processing time, low sample volume and reduced cost per test. Currently, Flow Cytometers are used for blood cells enumeration, however, they are expensive, requires fluorescent tagging of cells and trained technicians to operate the instrument. We propose a non-fluorescent microfluidic architecture with single excitation and detection scheme using the barcoded particles fabricated using Stop Flow Lithography process. The barcoded particles designed with specific number of coding regions can generate numerous distinct patterns of electrical signatures and can be used in biological assays to detect multiple blood cells.

A novel design of the asymmetric rectangular barcoded particle was proposed and tested in COMSOL Multiphysics. The barcoded particle with five coding regions generated distinct bi-polar signatures in the microfluidic impedance detection system. Different configurations of the sensing system were proposed to detect the conjugated microspheres (representative of blood cells) effectively based on the site of conjugation. The bottom co-planar electrode and top-bottom electrode configurations were tested for sensitive detection of conjugated microspheres to the barcoded particle. We found that our microfluidic detection system was sensitive enough to detect the presence of a microsphere attached to the

barcoded particle. Further, we also investigated the effect of microspheres conjugation orientation to the barcoded particle and their associated electrical signatures. We developed a multi-feature selection algorithm to solve the orientation problem and improved the accuracy of our sensing mechanism. Finally, we fabricated the microfluidic chips using lithography, and co-planar electrodes on glass surfaces using thin film deposition process in the clean room. Our proposed microfluidic system can enumerate multiple blood cells in a single assay using barcoded particles. The concentration of these cells provides useful information about disease onset and progression. Such sensors can be used for diagnostic and management of diseases like Sepsis, Acute Kidney Injury, HIV/ AIDS.

ACKNOWLEDGEMENTS

I would like to begin by thanking Dr. Umer Hassan for being a great mentor and giving me the opportunity to work under his guidance. His guidance proved invaluable through the course of my thesis project and my Masters Degree.

I would like to extend my special thanks to students of Dr. Zahn's lab at Rutgers University-Department of Biomedical Engineering for their support and valuable insights. I am also grateful to members of Biomedical Engineering Cleanroom at Rutgers University for assisting me in the fabrication processes.

I am thankful to Dr. Chung-Tse Michael Wu and Dr. Zoran Gajic for being a part of my Masters Thesis committee, whose feedback will be immensely helpful. Special thanks to all the members of my lab: Ahsan Sami, Corey Norton, Brandon Ashley, Kurt Wagner, Priya Parikh and Hammad Arshad for their contributions and timely help.

I would like to extend my thanks to John Scafidi, Arletta Hoscilowicz, Pamela Heinold, Christy Lafferty and Kevin Wine.

I would like to mention my parents for their constant support and keeping me motivated at all times. Finally, I am thankful to my friends and all the faculty who served as a constant motivation for me to excel.

TABLE OF CONTENTS

LIST OF FIGURES

CHAPTER 1
INTRODUCTION

1.1 Introduction to whole blood

Blood is a specialized fluid that circulates throughout the body to perform essential functions. It is comprised of four main components, namely plasma, red blood cells (RBC), white blood cells (WBC), and platelets. Plasma is the liquid component of the blood, RBC is about 40-45 percentage of blood, WBC is about 1 percent of the blood and Platelet are the blood cell fragments helpful in blood clotting. The average size of the Platelets is about 1-2 μm, RBCs is about 4-5 μm and WBCs are about 7-15 μm. The concentration of the blood cells changes during the onset and progression of disease [1]. The Complete Blood Cell Count (CBC) is ordered by medical professionals to monitor the patients response to disease [1]. Figure 1.1 shows the components of the whole blood. The blood cell expresses various proteins on its surface like CD4, CD8, CD64, CD11b and many others. These proteins provide a target for immunophenotyping of cells and are known as cell surface biomarkers. The study of cell surface biomarkers can provide patient specific details about disease onset and progression. The study of multiplexed biomarkers present in the blood sample can help us infer the state of the diseased individual.

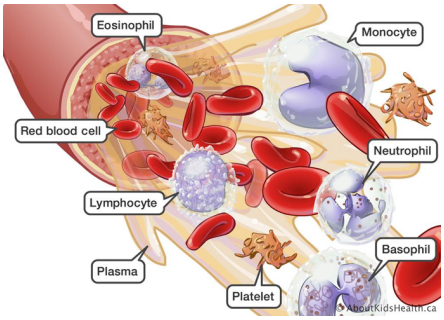

Figure 1.1: Components of whole blood. [2]

1.2 Flow cytometry

Flow Cytometry is commonly employed in clinical laboratory for obtaining characteristics of heterogenous cell population. It employs the optical method for finding out multiple physical and chemical characteristics of the cell population in a stream of fluid [3]. Its study is used in the identification and quantification of immune systems cells and characterization of hematological malignancies [4]. The information about cell size and internal structure of the cell can be inferred from scattering of light from different angles from the cells. Hence, its a very valuable tool for detailed qualitative and quantitative analysis of heterogenous cell population in an assay [3]. It is widely used for immunophenotyping of large variety of clinical samples like whole blood, bone marrow, cavity fluids, cerebrospinal fluid, urine and other solid tissues [3]. Figure 1.2 shows the image of the NovoCyte Benchtop Flow Cytometer by ACEA Biosciences.

Figure 1.2: NovoCyte Benchtop Flow Cytometer by ACEA Biosciences [5]

The laminar flow inside the cyclometer ensures that once cell passes through the interrogation point at a time where the laser light probes the cell and the emitted light is processed by the dichromatic mirror. The isolation of a wavelength is done by the dichroic mirror and the photodetectors detect the emitted light which are digitized by photodetectors for computer analysis. One of the photodetectors measures the scatter along the path of the laser, thus measuring the Forward Scatter (FSC), allowing the discrimination of cell by

size. The intensity of the voltage produced by the forward scatter is directly proportional to the diameter of the cell under interrogation. The emitted light ninety degrees relative to the laser is measured by the other photodetector, thus measuring the Side Scatter (SSC), providing information about the internal structure of the cell. The schematic of the Flow Cytometer is illustrated in Figure 1.3.

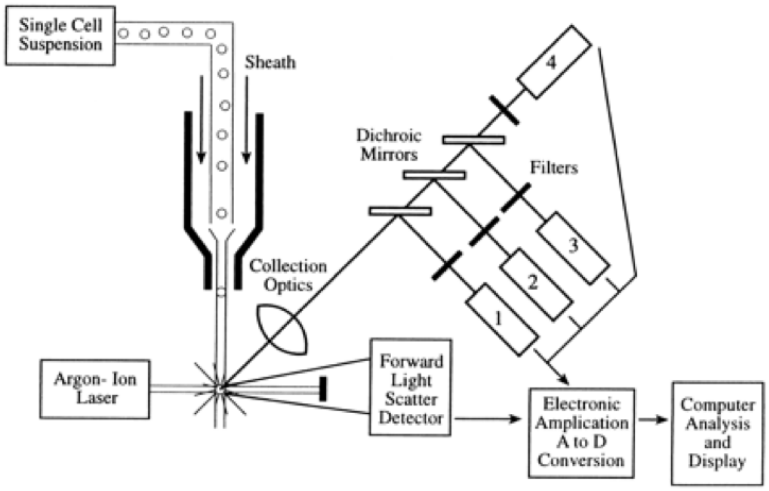

Figure 1.3: Schematic of Flow Cytometer [6]

1.3 Multiplexing

Initially, the analysis of multiple analytes in an assay was not a single step process. Back then, the multiple analytes present in the biological assay were analyzed one at a time. This method of analyzing the analytes had several disadvantages like large volume consumption of the sample and difficulty on detecting large number of analytes. The parallel quantification of multiple protein, nucleic acid sequence and cytokines gives an advantage to researchers and clinicians to obtain high density information in a minimal time along with low sample volume and cost [7]. The increase in the use of high throughput assays in biomedical field, including clinical diagnosis, and drug discovery requires the use of effective strategies for multiplexing. One of the effective strategies would be the usage of

barcoded particles that have the information encoded in them about their composition and thus enable identification.

1.3.1 Multiplexing techniques

There are various multiplexing techniques enables the detection of several biomarkers simultaneously in a single assay and hence enhances the clinical sensitivity and reliability [8]. The two broad technologies which are commonly used in multiplexing are Planar Arrays and Suspension Arrays [7]. Both of these techniques have application specific advantages. Planar arrays like DNA arrays and protein microarrays are best for the applications where ultra-high-density application is required [7].

Planar arrays are strictly dependent upon the positional encoding of the particles. In this method, the probe molecules are immobilized on the substrate which are then encoded by the coordinates of the particle position [9]. Suspension arrays use the barcoded particles for the attachment of probe and reaction. This method of multiplexing provides higher flexibility in analytes detection and very fast reaction kinematics [10].

There are variety of encoding schemes available for the Suspension arrays like spectrometric, graphical, electronic and physical. The spectrometric uses specific wavelengths of light for encoding and radiation like fluorophores, photonic structure and Raman tags are used for species identification [11]. The spectrometric encoding scheme has a limitation on the number of barcodes available due to spectral overlap. Graphical barcode use the patterned optical elements on a micro carrier like striped rods, dot patterned particles and ridged particles. There exists a limitation on the identification of these patterns encoded by graphical technique as they can be only distinguished when target signals florescence is sufficiently high [7]. Also, radio frequency memory tags can be used for species identification and it generates nearly unlimited number of barcodes [12]. However, synthesis of these carriers may prove to be expensive and slow. All the above proposed multiplexing techniques have

some or the other disadvantage.

Doyle and his colleagues have developed a multiplexing technique based on the laminar flow of microfluidics to synthesize multifunctional particles which have distinct region of analyte encoding and target capture [7]. The particles generated had fluorescent graphically coded region and probe loaded region, synthesized in a single step. These particles enhanced the specificity and sensitivity of the analyte detection. Dot coding scheme was used to generate near about 220 codes. So, in general the techniques which are used in multiplexing are optical based and electrical impedance-based techniques.

Optical method of multiplexing technique provides a high throughput multiplexing with high sensitivity. The high sensitivity is enabled by the use of different methods of barcoding for the barcoded particles. However, the optical method has a limited by the large size of the detection instrument [13]. In comparison to optical method, the electrical impedance method offers advantage of being lightweight, ultra-compact, low power, and high sensitivity.

1.3.2 Multiplexed biomarker study

In recent days there has been a lot of emphasis on the development of protein-based diagnosis that provides an increased level of information about the biomolecular detail and the state of disease. For instance, there is an investigation being conducted on the biomarkers for generating personalized and effective treatment of cancer [14]. Although there has been a significant work being done in the field of discovery of biomarkers and its panels, yet this technology has not been deployed commercially.

Even today in clinical settings, the immunoassay relies on detection of one biomarker at a time [15]. In present times, there has been a lot of emphasis on the development of technology that has the ability of detecting multiple protein target molecules from a single sample. The bead- based Luminex platform has been commercially very successful in

doing so [15]. Various micro and nano scale fabrication technologies has been utilized to develop multiplexed sensor arrays to quantify various target molecules parallelly in a single sample.

A scalable silicon photonic platform configurable into a multiplexed detection array to quantify multiple protein molecules at a particular time, was developed at University of Illinois at Urbana Campaign [15]. The multiplexed detection array utilized the change of reflective index of the sensors surface to quantify the presence of various analytes. The array of silicon photonic sensors was used in rapid and simultaneous detection of eight cancer biomarkers in blood serum. The time of detection of eight biomarkers was estimated one hour. The mirroring resonators in the multiplexed sensor array offered a unique real time monitoring capability. This feature was extremely useful in assay development time as each and every step of the assay caused a shift in the resonance wavelength [15].

Microarrays are well suited for the multiplexed assay analysis, but they are limited in their scope because of its slow speed, less sensitivity and being more expensive [16]. With the advancement of studies in the field of disease related biomarkers, it become really important that robust diagnostic technology is developed. This technology is not only cost effective but also provides a rapid detection of multiple biomarkers from a single patient sample. The multiplexed diagnostic can provide a more detailed view of the biomolecular dynamics which gives deep understanding about the onset and progression of the disease [17]. Multiplexed analysis of assay also provides in depth understanding of the role of the microRNA (miRNA) molecules. The multiplexed analysis also points towards the application of miRNA molecules in the regulation of the protein expression [18]. Unfortunately, due to technological gap, the multiplexing of miRNA molecules has not been extended to clinical settings [19].

1.3.3 Recent advancements in biomarker study

Recently a technique has been developed which exploits the advantages of target specific amplification and multiplexed detection using mirroring resonators to generate a profile of multiple miRNA from clinical samples [16]. The silicon nanowire field effect (SiNW-FET) device has been developed to carry out the multiplexed electrical detection of lung cancer biomarker [20]. The SiNW arrays were fabricated using the photolithography and the anisotropic wet chemical etching with tetra-methylammonium hydroxide (TMAH) and have the advantage of being low cost and mass reproducibility [20]. The SiNW nanosensor was then attached to the PDMS microfluidic device which enabled the multiplexed detection using a very small volume of sample. The PDMS microfluidic chamber was used to supply sufficient number of molecules onto the surface of the nanowire FET sensor to enable sensing. With the help of silicon-based nanowire field device, the biomarkers for the lung-based cancer namely miRNA-126 and carcino embryonic antigen (CEA) was quantified in a multiplexed manner with high sensitivity and specificity. CEA is a very valuable biomarker as its generated in early stages of lung cancer. Thus, this technology has the utility of detecting and diagnosing cancer in the early stages. This microfluidic system provides main advantages over the existing multiplexed technology. These advantages included the presence of a local positioning detection system that enabled multiplexed detection, small consumption of reagents, improved throughput and reproducibility [20]. The biosensor demonstrated a rapid and sensitive detection of as low a concentration of 0.1fM for miRNA-126 and 1fg/ml CEA with good specificity [20]. There are several strategies for cancer biomarker detection that has been proposed before like blotting (Koscianska et al., 2011; Morita et al., 1998), electrochemical transduction (Hamidi-Asl et al., 2013), polymerase chain reaction (PCR) (Chen et al., 2005; Raymond et al., 2005; Schmittgen et al., 2004;), surface plasmon resonance (Sipova et al., 2004;) and various others.

These methods have several disadvantages associated with them like low sensitivity, inefficient multiplexed detection, time consuming and expensive equipment. So, in comparison

to these technologies, silicon nanowire field effect (SiNW-FET) device is a low cost and more sensitive alternative for multiplexed biomarker detection.

Also, work has been done in the field of multiplexed detection of small molecules and a universal aptameric system has been developed [21]. This aptameric system took advantage of double stranded DNA/perylene diimide (dsDNA/PDI) which was used as the probe to detect small molecules. Aptamers are single stranded DNA or RNA molecules and they get selected in vitro by a process known as systematic evolution of ligands by exponential enrichment. During this approach, a new kind of PDI was synthesized which could quench double stranded DNA fluorophores with a high quenching efficiency. The broad spectrum of quencher was then exploited to develop a multicolor biosensor. The biosensor had higher sensitivity towards smaller analytes due to high quenching efficiency and autocatalytic target recycling amplification. Also, multiplexed analysis of various small analytes was possible from a homogenous solution. This provided an added advantage that rapid screening of multiple biotargets could be performed simultaneously [21]. In recent years there has been a considerable increase in the demand of point-of-care (POC) multiplexed diagnostic assays [22].

Earlier the paper based lateral flow devices (LFDs) were regarded as low cost solution for disease diagnosis for POC applications. On similar lines, multi path LFD was developed for multiplexed analysis of analytes. Multiplexed analysis of the assay was done using multipath lateral flow device (LFD) using laser direct-write (LDW) technique. The multiple flow paths present in the LFD device, enabled simultaneous detection of multiple analytes in the different parallel channels without any cross reactivity between them. The liquid sample containing the analytes moved because of the capillary action through the different zones in the paper strip. During this transport of the analyte in the paper, they get to interact with different antibodies and hence bind to them. These antibodies were deposited onto the paper initially, the interaction between antibodies and analytes causes it to be captured in the detection region which is marked by the test line and the control line. The detec-

tion of the analyte is governed by the color code in the test region and the color coding of the control region ensures that the sample flow is complete through the device and that the device is working correctly. The laser which was employed in the LDW process was a 405 nm continuous wave diode laser with a maximum output power of 110mW. The LFD device was successful in multiplexed detection two inflammation-based markers namely C-reactive protein (CRP) and Serum amyloid A-1 (SAA1) which is used in diagnosis of bacterial infections.

These LFD devices have an added advantage of being low cost, ease of producibility, and have resulted expansion in various sectors like hospitals, clinical laboratories, home and physicians office [22]. These days significant work has been done to develop homologous and high-throughput multi-wavelength fluorescence polarization immunoassay (MWFPIA) for the detection of multiplexed mycotoxins [23]. Multi- analyte immunoassay has received an increasing attention due to their innate advantages like short assay time, low sample consumption and reduced detection cost per assay.

1.4 Statement of problem

The Flow Cytometry is being used to perform multiplexing and characterization of heterogenous cell population. It is being used in the clinical setting to characterize the physical and chemical properties of the cell population under study. However, usage of Flow Cytometer is disadvantageous; they are bulky, expensive, require fluorescent tagging of cells, high maintenance and trained technicians for operation.

Therefore, there arises the need to develop a low cost, compact, portable device to perform multiplexing. In this work, our main objective is to design, test and fabricate the parts of the microfluidic system to perform multiplexing.

The non-fluorescent microfluidic impedance-based multiplexing system has advantages of being label-free, inexpensive, single excitation and detection source and the ability to per-

form extensive multiplexing. The microfluidic detection system has an added advantage of consuming less sample volume and being able to be miniaturized into small device.

1.5 Thesis organization

Chapter 2 presents an overview of the novel approach to perform multiplexing through non fluorescent microfluidic detection system. We briefly touch upon what an impedance-based detection system is and then describe our proposed architecture for the multiplexing of blood cells. After investigating the proposed design of the novel barcoded particle utilized for multiplexing, we discuss the motivation of the design and various design characteristics.

Chapter 3 focuses on the testing of the various designed components in the COMSOL Multiphysics software. First, we discuss the testing of the designed asymmetric barcoded particle with different number of coding regions. In subsection 3.2, we test the conjugation of microspheres to the barcoded particle. The microspheres were conjugated at different sites on the barcoded particle and their corresponding electrical signatures were observed. Subsection 3.3 talks about the proposed top-bottom electrode configuration for sensitive detection of microspheres conjugated to barcoded particles for analysis of multiplexed assays.

Chapter 4 presents the fabrication recipe for various components in the non-fluorescent microfluidic detection system. Finally, Chapter 5 discusses the conclusion and future scope. We discuss on how this novel approach for multiplexed detection can be improvised and the further studies that can be performed on the proposed detection system.

CHAPTER 2

MICROFLUIDIC DETECTION SYSTEM

2.1 Impedance based microfluidic detection system

Impedance based microfluidic detection system is an electrical analysis of the heterogeneous cell population. The blood cell population flows over the co-planar electrodes fabricated in the microfluidic channel. The co-planar electrode system is given an AC voltage signal and passage of cells over the electrodes disrupts the electric field. The increase in the impedance between a pair of electrodes is measured and differential bi-polar pulse is generated. For instance, Figure 2.1 shows the side view of the microfluidic impedance detection system. The microfluidic system comprises of three co-planar electrodes A, B and C. The central electrode B, is excited by 10 V AC signal and the impedance measurement is done between A and B electrode pair. The image also describes the bi-polar pulse generated between the co-planar electrodes after measurement. The differential bi-polar pulse generated which helps in characterization of heterogeneous cell population.

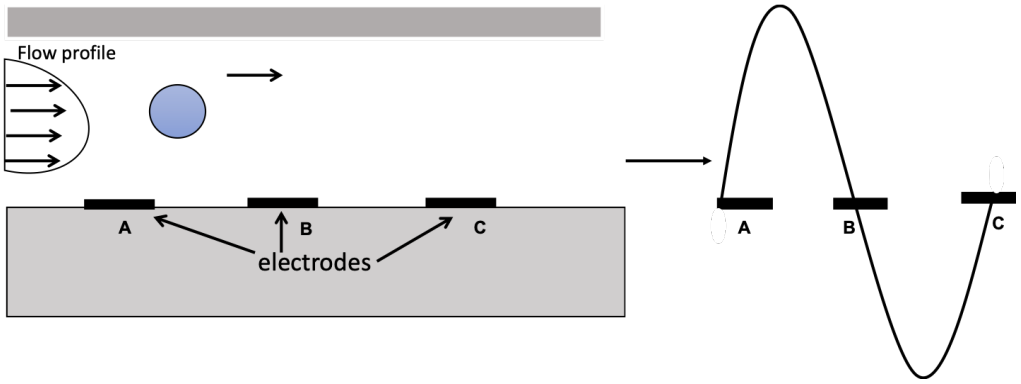

Figure 2.1: Side view of microfluidic impedance detection system and the generated bi-polar pulse of impedance detection system.

Probing the cell population at different frequencies can help us obtain useful information about cell size and internal structure. At low frequencies, the cell membrane acts as a

barrier to current flow and the impedance amplitude provides the cell size [24]. At intermediate frequencies, impedance measurement gives information about the membrane properties [24]. At high frequencies, the membrane is minimally polarized, and the impedance measurement provides information about the internal cell structure [24]. Thus, the microfabricated impedance-based detection system can detect, count and analyze the cell size by combining the concepts of microfluidics and electronics. The system is low cost, small size and portable solution for cell analysis and characterization. Multifrequency impedance measurement can further give insight into cell differentiation based on internal cell structure.

2.2 Microfluidic architecture for blood cell multiplexing

The proposed architecture for the detection of single blood cell in the microfluidic channel comprises of the channel and the micro fabricated co-planar electrodes. The detection system consists of a set of three co-planar electrodes. The width and the spacing between electrodes are maintained at 8 μm. The microfluidic channel has a cross-section of 50 (height) x 100 (width) μm^2. The excitation voltage of 10 V AC is provided to the central electrode and the impedance measurement is done between the pair of extreme electrodes. As the cell passes over the co-planar electrodes, the electric field lines are disrupted, and the impedance measurement is performed. The differential bi-polar pulse is generated to reject the common mode noise. Figure 2.2 shows the schematic of the proposed microfluidic architecture for single cell detection.

To test the proposed design, a blood cell of size 10 μm is flown in the microfluidic architecture. The architecture is simulated in COMSOL Multiphysics to generate the electrical signature for the blood cell. The microfluidic architecture is sensitive enough to detect the presence of a single cell in the channel. Figure 2.3 illustrates the electrical signature of the single blood cell flowing in the microfluidic architecture.

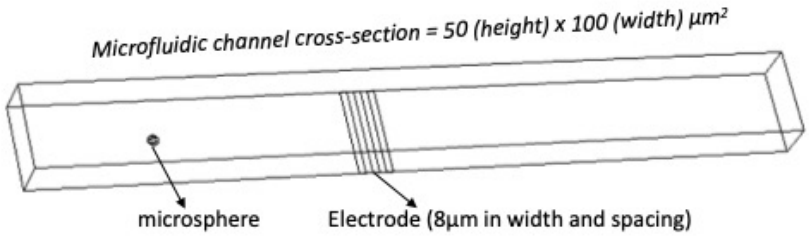

Figure 2.2: Schematic of architecture for blood cell multiplexing.

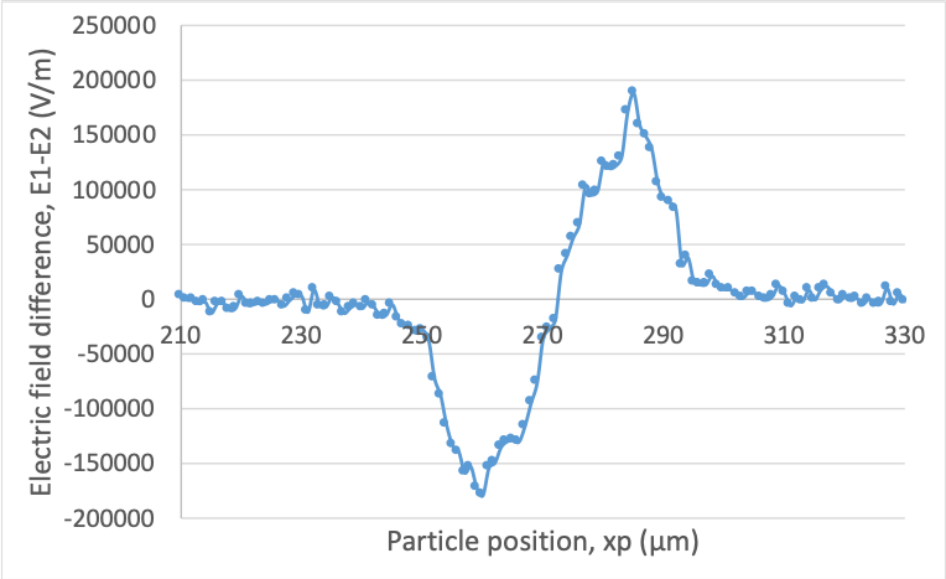

Figure 2.3: Electrical signature of the microsphere in microfluidic architecture.

2.3 Design of barcoded particle

The inspiration for the design of the unique particle for multiplexing, came from barcode. The barcode is a visual method for representation of data by variation of the width and spacing between the parallel lines. We propose a novel design of asymmetric barcoded particle with certain number of coding regions which generate distinct electrical signature in the microfluidic architecture. The presence and absence of coding regions generate large number of distinct signatures and hence make multiplexing of blood cells possible. Figure 2.4 illustrates the top view of the barcoded particle with five coding regions. The dimension of the barcoded particle is 250 (length) x 30 (thickness) x 70 (height) μm^3. The spacing

between the two consecutive coding regions is 40 μm, the width of the barcode is 12 μm and the height is maintained at 50 μm.

The barcoded particles are fabricated by the method of Stop Flow Lithography [25]. In this method, the particles are synthesized in a stationary monomer film in the PDMS channel, before being flushed out [25]. The cyclic repetition of this process leads to generation of an array of the barcoded particles.

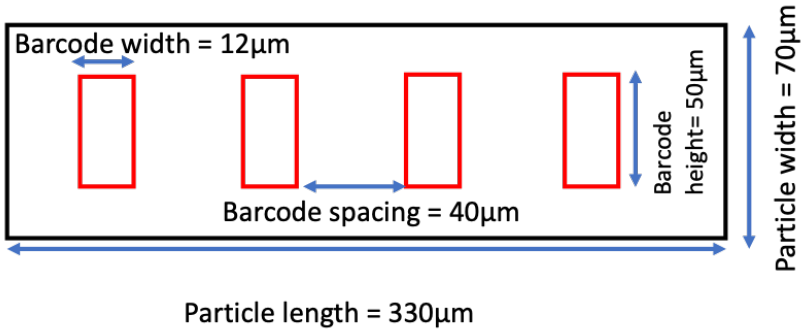

Figure 2.4: Top view of the barcoded particle with four coding regions

CHAPTER 3

DEVICE TESTING

3.1 Testing of barcoded particle

The designed barcoded particles with four and five coding region are simulated in COMSOL Multiphysics. Figure 3.1 and 3.2 illustrates the top view of the barcoded particle with five and four coding regions respectively.

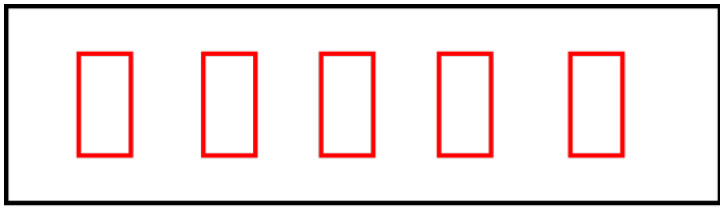

Figure 3.1: Top view of the barcoded particle with five coding regions

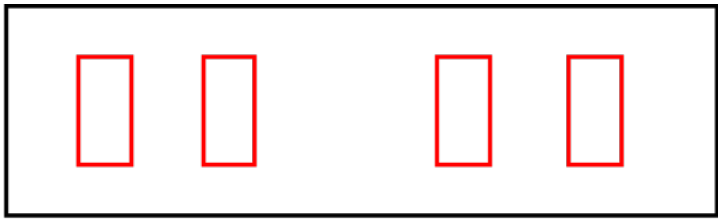

Figure 3.2: Top view of the barcoded particle with four coding regions

The rectangular asymmetric barcoded particles are flown in the microfluidic channel consisting of three co-planar electrodes. The co-planar electrodes are fabricated at the bottom of the microfluidic channel. Figure 3.3 and 3.4 shows the barcoded particle in the

microfluidic channel.

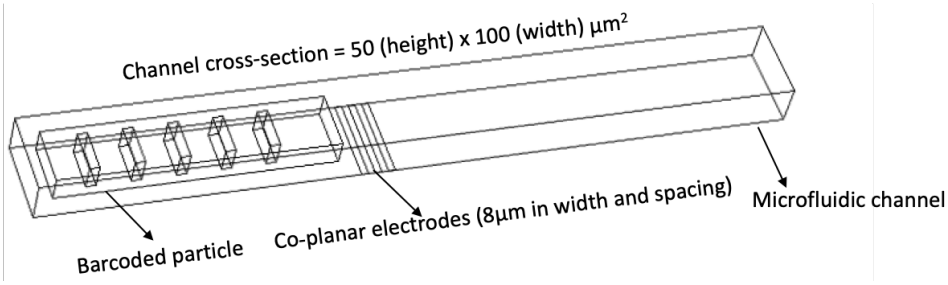

Figure 3.3: Cross sectional view of the microfluidic architecture

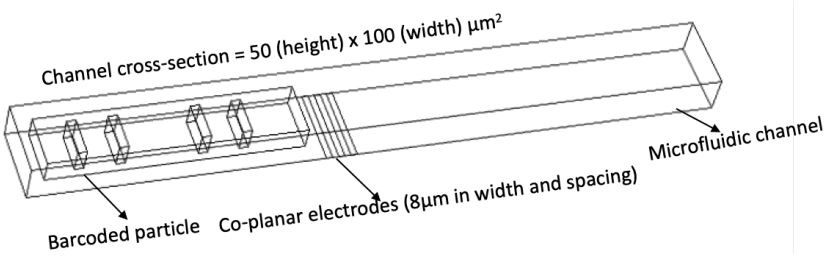

Figure 3.4: Cross sectional view of the microfluidic architecture

While flowing through the microfluidic architecture, each barcoded particle generates a distinct electrical signature which comprises of distinct entry and exit pulse, along with the certain number of maxima. The number of maxima in the electrical signature is representative of the number of coding region in the barcoded particle. For instance, the barcoded particle with five coding regions has five maxima in the electrical signature. Figure 3.5 and 3.6 presents the electrical signatures produced by the barcoded particle with five and four coding regions respectively.

3.2 Microsphere conjugation at bottom of barcoded particle

A single microsphere (representative of blood cell) is conjugated to the barcoded particle. The size of the microsphere conjugated is in the diameter range of 7 to 12 μm. The study

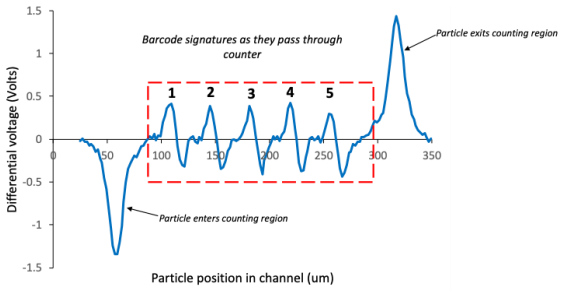

Figure 3.5: Electrical signature of the barcoded particle

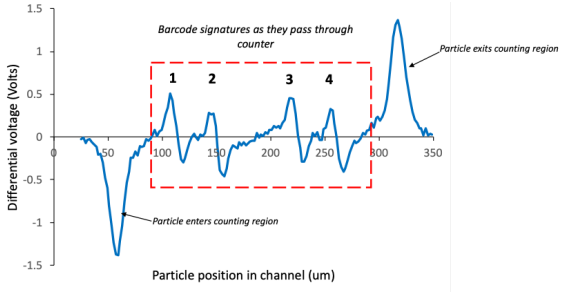

Figure 3.6: Electrical signature of the barcoded particle

is performed in COMSOL Multiphysics to test the sensitivity of the proposed microfluidic architecture. We intend to analyze and check the sensitivity of the proposed system to the detection of a single microsphere conjugated to the barcoded particle. Figure 3.7 shows the top view of the barcoded particle conjugated with a single microsphere. Also, Figure 3.8 presents the cross-sectional view of the microfluidic channel with the conjugated barcoded particle. It is observed that when a 12 μm microsphere is conjugated, the percentage change in the electrical signature is 3.5 times the original electrical signature of the barcoded particle (with no microspheres conjugated). Also, when a 10 μm microsphere is conjugated then percentage change in electrical signature is nearly twice the original. However, the change is 0.32 times the original when 7 μm microsphere is conjugated. The electrical signatures of the microspheres conjugated to the barcoded particle can be observed in Figures 3.9, 3.10 and 3.11. Hence, by observing the electrical signatures we can make a comment that proposed microfluidic architecture is sensitive to the detection of a single microsphere conjugated to the barcoded particle.

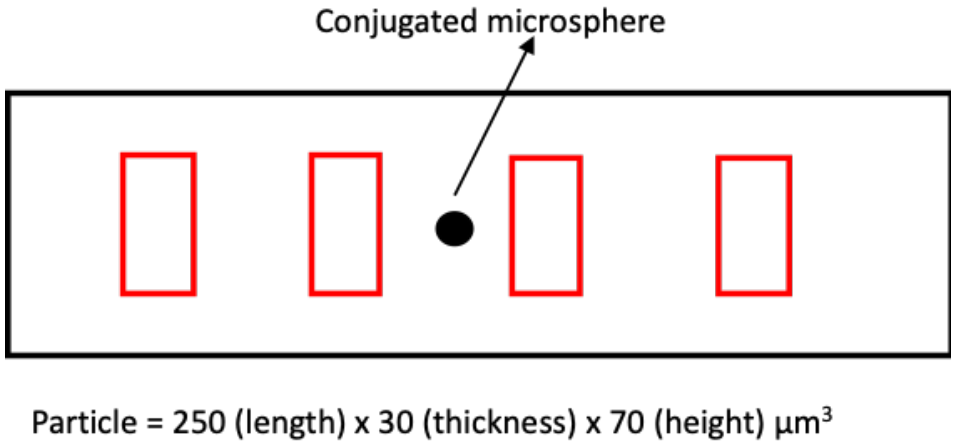

Figure 3.7: Top view of the barcoded particle with microsphere

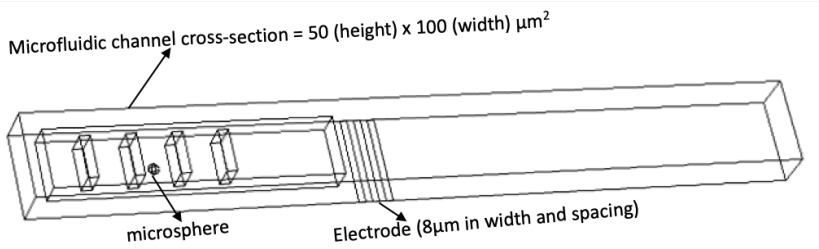

Figure 3.8: Cross sectional view of the microfluidic architecture

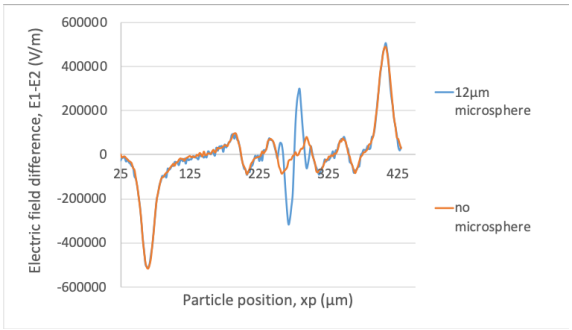

Figure 3.9: Electrical signature of conjugated microsphere of 12 µm

3.2.1 Orientation of conjugated microsphere

The orientation of the conjugated microspheres at the bottom of the barcoded particle is further studied. We are interested in observing if the orientation of the microsphere con-

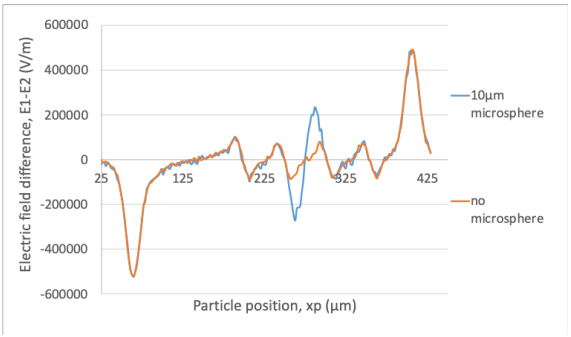

Figure 3.10: Electrical signature of conjugated microsphere of 10 µm

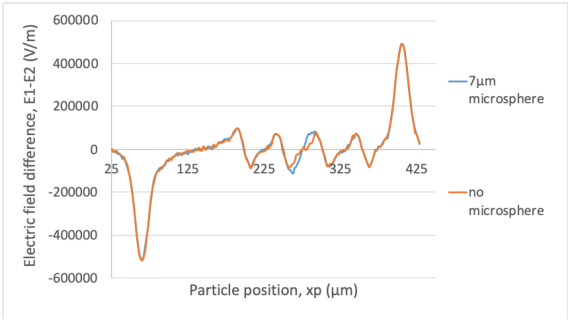

Figure 3.11: Electrical signature of conjugated microsphere of 7 µm

jugation has any effect on the electrical signature. An array of microsphere is conjugated at the bottom surface of the barcoded particle in different possible orientations. We start by conjugating 2 microspheres in a row of 10 µm in diameter (1x2 microsphere array) at the bottom surface of the barcoded particle. Figure 3.12 and 3.13 show the top and cross-sectional view of the barcoded particle and microfluidic architecture respectively. It is observed that the percentage change in the electrical signature of the conjugated 1x2 microsphere array is 3 times the original signature of the barcoded particle (with no microsphere conjugated). The width of the pulses in the electrical signature is 26 µm. Figure 3.14 presents the electrical signature of the barcoded particle conjugated with 1x2 microsphere array.

Further, the orientation of the conjugated microsphere is changed to conjugate an array of two microspheres of 10 µm in diameter in diagonal fashion at the bottom surface of the

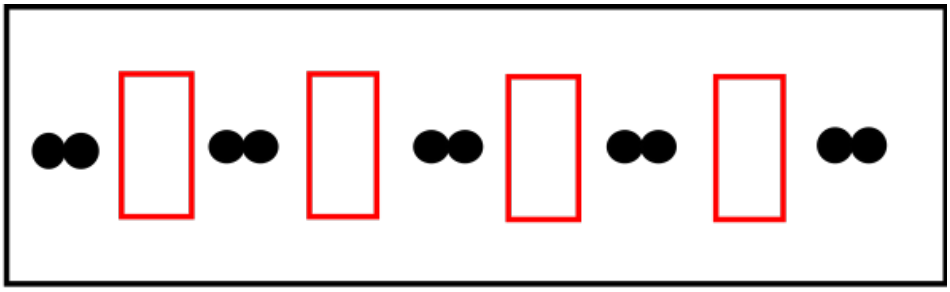

Figure 3.12: Top view of the barcoded particle with 1x2 microspheres

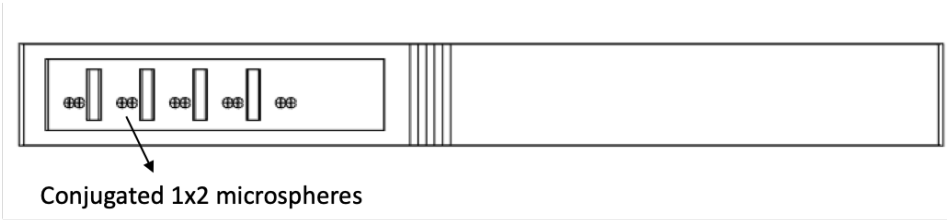

Figure 3.13: Cross-sectional view of the microfluidic architecture

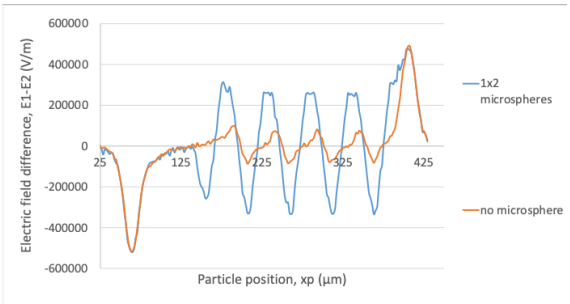

Figure 3.14: Electrical signature of 1x2 microsphere array conjugated

barcoded particle. Figure 3.15 and 3.16 illustrate the top and cross-sectional view of the barcoded particle and microfluidic architecture respectively. The percentage change in the electrical signature of the conjugated array of microspheres in the diagonal fashion is 4.6 times the original signature of the barcoded particle (with no microsphere conjugated). The width of the pulses in the electrical signature is 28 µm. Figure 3.17 presents the electrical signature of the barcoded particle conjugated with the microsphere array in diagonal fashion.

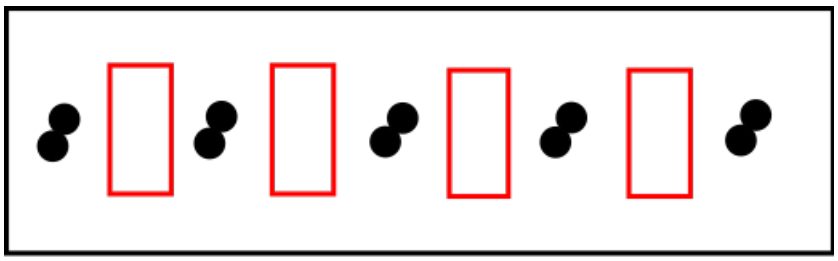

Figure 3.15: Top view of the barcoded particle with 2x1 diagonal microspheres

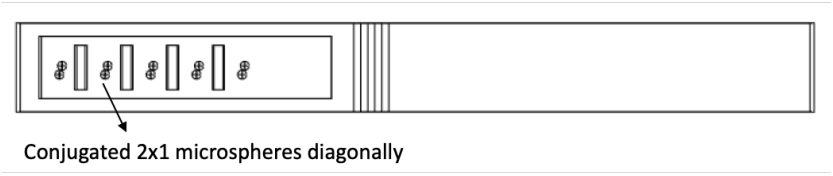

Figure 3.16: Cross-sectional view of the microfluidic architecture

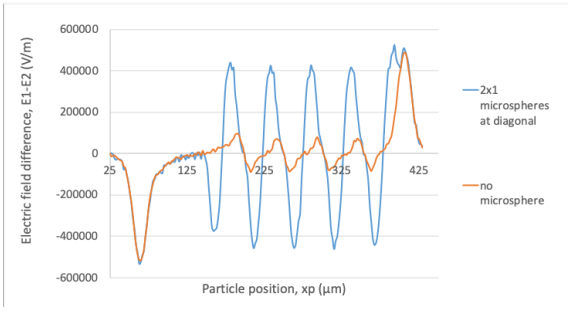

Figure 3.17: Electrical signature of 2x1 diagonal microsphere conjugated

The orientation of the conjugated microsphere is further changed for our study. Now, two microspheres of 10 µm in diameter (2x1 microsphere array), stacked on top of each other, are conjugated. Figure 3.18 and 3.19 illustrate the top and cross-sectional view of the barcoded particle and microfluidic architecture respectively. As shown in Figure 3.20, the percentage change in the electrical signature of the conjugated array of microspheres is 4.8 times the original signature of the barcoded particle (with no microsphere conjugated). The width of the pulses in the electrical signature is 30 µm.

Hence, it can be observed that orientation of the conjugated microsphere has an effect on the associated electrical signature. When stacked microspheres are conjugated at the

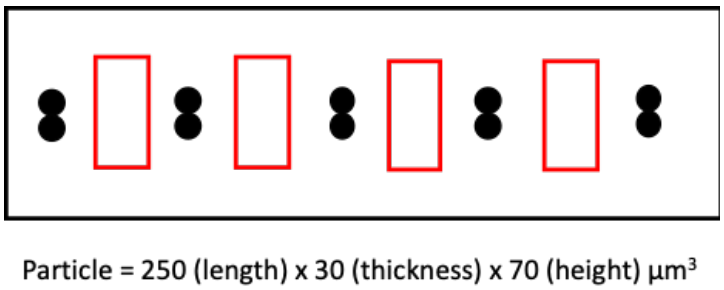

Figure 3.18: Top view of the barcoded particle with 2x1 microspheres

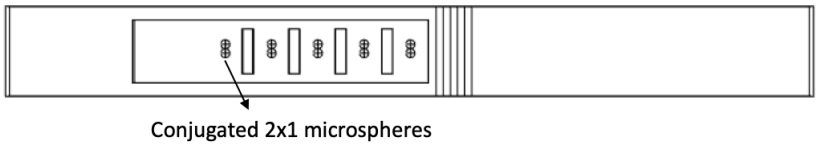

Figure 3.19: Cross-sectional view of the microfluidic architecture

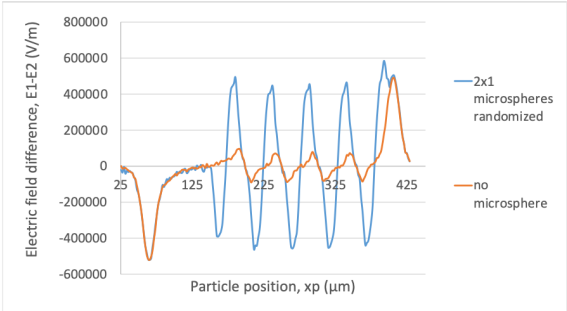

Figure 3.20: Electrical signature of 2x1 microsphere conjugated

bottom surface of the barcoded particle then the distinctive change in the electrical signature is observed. Also, pulse width is an important parameter indicative of the orientation of the conjugated microspheres. The separation between the coding regions of the barcoded particle can be controlled to decide the number of microspheres to be conjugated.

3.3 Microsphere conjugation at the top of barcoded particle

The microsphere array is conjugated at the top surface of the barcoded particle to check the sensitivity of the microfluidic detection system. For this study, two microspheres of 10 µm in diameter are stacked on top of each other. The barcoded particle with the conjugated

microspheres is then flown in the microfluidic architecture to obtain the electrical signature. However, the electrical signature of the barcoded particle didn't reflect any significant change compared to the situation when no microspheres are conjugated to the barcoded particle. The detection system (micro fabricated co-planar electrodes) does not detect the presence of the microspheres attached at the top surface of the barcoded particle. The detection system is present at the bottom surface of the microfluidic channel and hence is insensitive to the microspheres conjugated to the top of the barcoded particle. Therefore, it is imperative to design the microfluidic architecture that could detect the presence of microspheres conjugated either on the top or bottom surface of the barcoded particle.

Figure 3.21 shows the cross-sectional view of the barcoded particle in the microfluidic architecture and Figure 3.22 presents the electrical signature obtained.

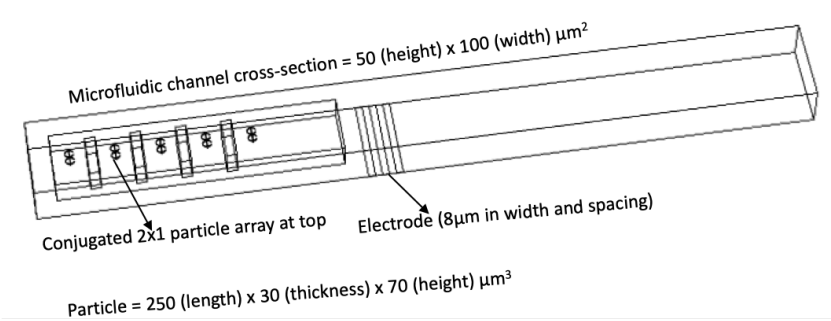

Figure 3.21: Cross-sectional view of the microfluidic architecture

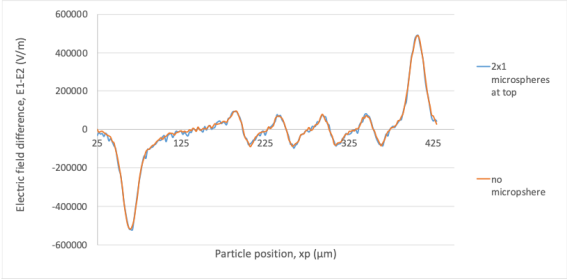

Figure 3.22: Electrical signature of the microspheres at the barcoded particle top

3.4 Testing of top-bottom electrode configuration

We propose a novel top-bottom sensing architecture which detects cells conjugated to the barcoded particle. The architecture discerns the presence of cells regardless of its site of conjugation. This microfluidic architecture comprises of top and bottom co-planar electrode system. There exist three co-planar electrodes which are micro fabricated both at the top and bottom surface of the channel. Each of the co-planar electrode set up is excited with an AC voltage of 10V and the impedance measurement is done between a pair of extreme electrodes. Figure 3.23 illustrates the cross-sectional view of the microfluidic architecture with top and bottom co-planar electrodes. Since each set of co-planar electrodes located

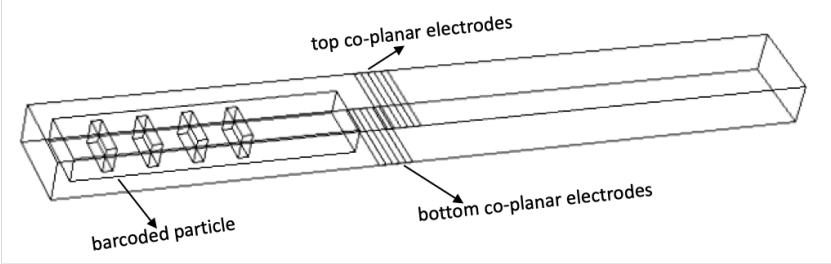

Figure 3.23: Cross-sectional view of the top-bottom microfluidic architecture

at the top and bottom works independently, the need to align the top and bottom co-planar electrodes w.r.t each other, in the microfluidic channel, is ruled out. The top and bottom co-planar electrodes are sensitive to the detection of microspheres attached at the top and bottom of the barcoded particle respectively. The differential electric fields (E1-E2) is measured at the bottom pair of electrodes and (E3-E4) is measured at the top pair of electrodes. The high amplitude of (E1-E2) differential electric field indicates that microspheres are conjugated at the bottom surface of the barcoded particle. However, when microspheres are conjugated at the top surface of the barcoded particle then (E3-E4) differential electric field has a high amplitude.

3.4.1 Microsphere conjugation at the bottom of the barcoded particle

For this study, an array of microspheres (two stacked microspheres) of 10 µm in diameter is conjugated all over on the bottom surface of the barcoded particle. The barcoded particle along with the conjugated microsphere is flown in the top-bottom microfluidic architecture to measure the differential electric fields. Figure 3.24 shows the cross-sectional view of the microfluidic architecture with the barcoded particle. It is observed that the amplitude of differential electric field (E1-E2) is higher than (E3-E4) for microspheres conjugated at the bottom surface. The differential electric field (E1-E2) is measured at the bottom pair of electrodes while (E3-E4) is measured at top pair of co-planar electrodes. Figure 3.25 presents the electrical signature obtained.

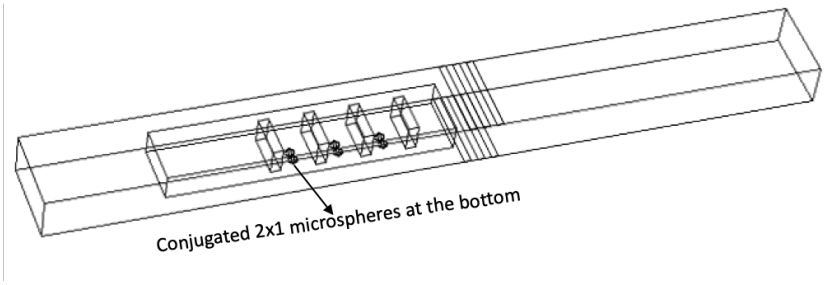

Figure 3.24: Cross-sectional view of the microfluidic architecture

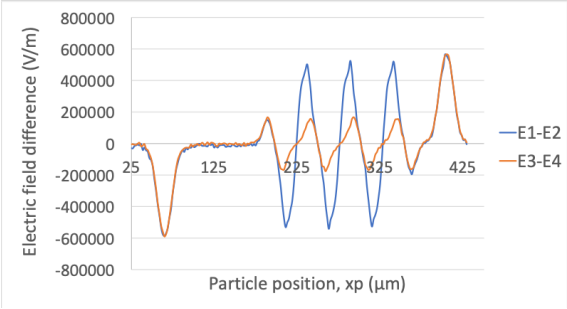

Figure 3.25: Electrical signature for microspheres conjugated at the bottom

3.4.2 Microsphere conjugation at the top of the barcoded particle

For this study, an array of microspheres (two stacked microspheres) of 10 µm in diameter is conjugated all over on the top surface of the barcoded particle. The barcoded particle along with the conjugated microsphere is flown in the top-bottom microfluidic architecture to measure the differential electric fields. Figure 3.26 shows the cross-sectional view of the microfluidic architecture with the barcoded particle.

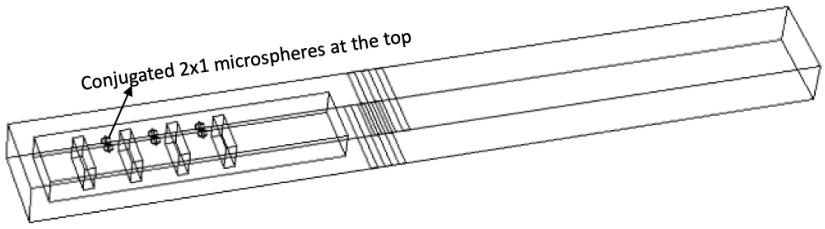

Figure 3.26: Cross-sectional view of the microfluidic architecture

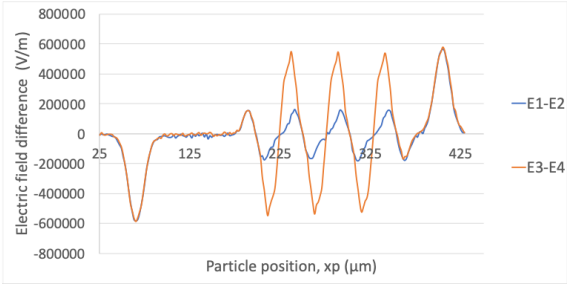

Figure 3.27: Electrical signature for microspheres conjugated at the top

It is observed that the amplitude of differential electric field (E1-E2) is less than (E3-E4) for microspheres conjugated at the top surface. The differential electric field (E1-E2) is measured at the bottom pair of electrodes while (E3-E4) is measured at top pair of co-planar electrodes. Figure 3.27 presents the electrical signature obtained.

CHAPTER 4
PRELIMINARY FABRICATION RESULT

4.1 Fabrication of barcoded particle

The asymmetric rectangular barcoded particle is fabricated using the Stop- Flow Lithography (SFL) method [25]. In this method, the particles are synthesized in a stationary monomer film present in the PDMS channel before being flushed out. The repetition of this step in a cyclic fashion yields large number of particles. Devices are fabricated by pouring PDMS on a silicon wafer containing channels patterned in the SU8 photoresist. The thickness of PDMS is maintained as 5mm or greater [25].

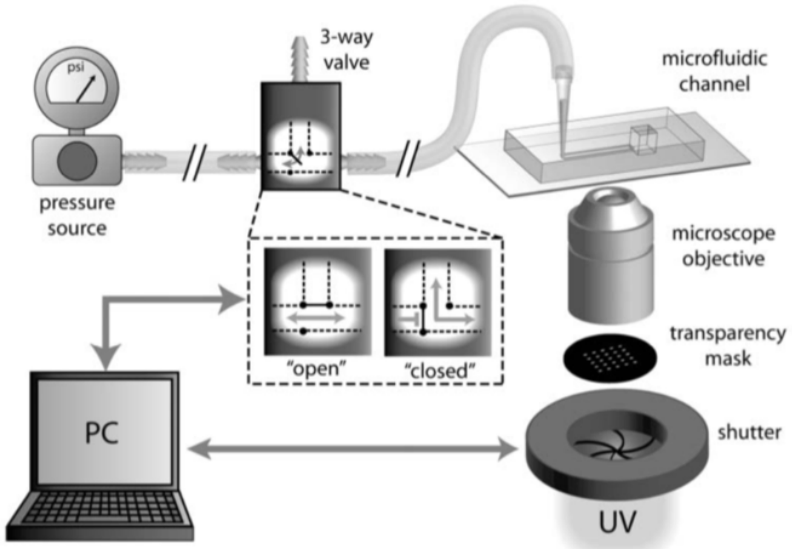

Figure 4.1: Stop Flow Lithography (SFL) set-up [25]

The fabrication of barcoded particle majorly consists of three phases. The first phase is the Stop phase where no external pressure is applied. The second stage refers to the Polymerize phase where an array of microspheres is polymerized in the PDMS channel

during which no external pressure is applied. The third and the last stage is the Flow phase where the polymerized particles are flushed out of the PDMS channel by applying external pressure. The deformation of PDMS channel due to application of external pressure causes the fabricated particles to be expelled out of the channel [25]. Figure4.1 shows the Stop Flow Lithography (SFL) setup. The Stop Flow Lithography (SFL) method generates high resolution asymmetric particles with high throughput.

4.2 Fabrication of microfluidic device

Standard photolithography on 3 glass wafer is performed in the fabrication of the microfluidic device. The microfluidic device is fabricated with three focusing channels for proper alignment of the fabricated asymmetric rectangular particles in the microfluidic architecture.

The first step in the process is to photo-pattern the resist on the silicon wafer. This includes cleansing the wafer, spin coating of SU8-2050 photoresist on the wafer and soft bake of the spin coated photoresist at 65 °C and 95 °C for 2 and 4 minutes respectively. Further, the wafer is UV Exposed via Chromium mask with exposure dose being 30 mJ/cm^2. The Post exposure bake is done as two-step process and it performed at 65 °C and 95 °C for 2 and 6 minutes respectively. Development of the exposed wafer is done in SU8 2050 developer solution for 7.5 minutes. At last, the wafer is rinsed, dried and hard baked. Figure 4.2 illustrates the steps involved in the fabrication of microfluidic device. Figure 4.3 shows the image of the microfluidic device. Further, the Soft Lithography is performed to form the PDMS microfluidic devices and bond them to the glass slide. Figure 4.4 summarizes the steps involved in Soft Lithography.

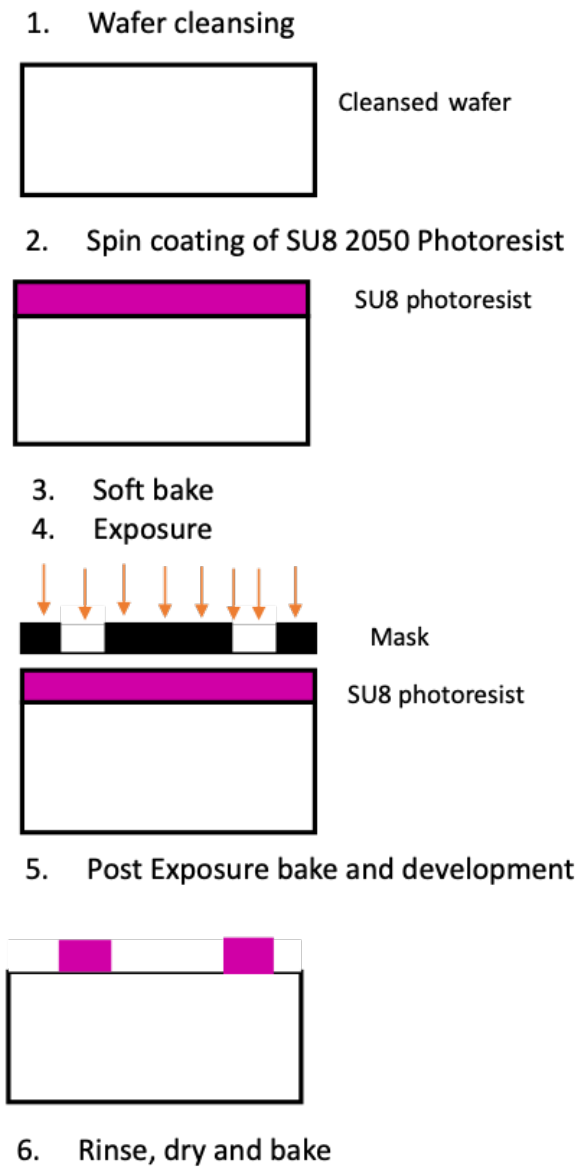

Figure 4.2: Process involved in microfluidic device fabrication

4.3 Fabrication of bottom electrodes

Standard photolithography is performed on 3 silicon wafer to fabricate the microelectrodes. The first step is to spin coat the HDMS layer to promote adhesion, followed by the coating of Shipley S1818 photoresist on the silicon wafer. The soft bake of the spin coated photoresist is then performed at 120 °C for four minutes. Further, the wafer is UV Exposed via Chromium mask with exposure energy being 350 mJ/cm^2. The Post exposure bake is done

Figure 4.3: Image of microfluidic device

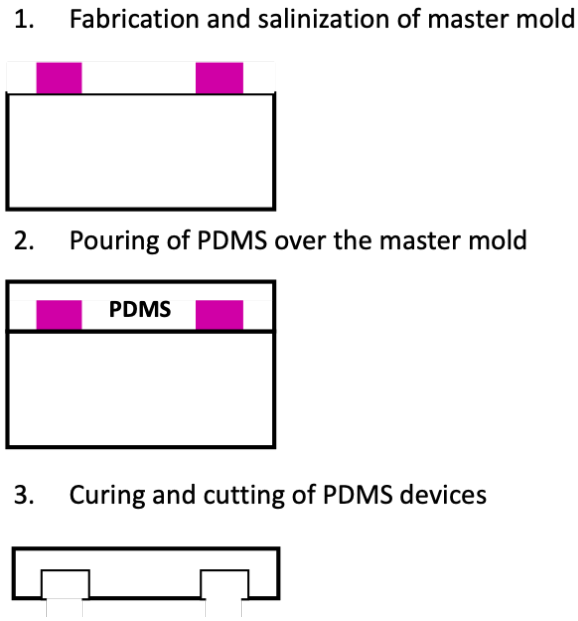

Figure 4.4: Process involved in soft lithography

as performed and development of the exposed wafer is done in MF139 developer solution for 4minutes. The photo patterning step is followed by deposition of 100nm Gold via electron beam evaporation on the wafer. A 10nm of Chromium layer is deposited to improve the adhesion of the gold layer on the substrate. In the final stage Lift-off is performed to complete the fabrication of Gold microelectrodes. The Gold metal is used to fabricate the electrode as it is an inert metal and resistant to corrosion. Figure 4.5 depicts the steps involved in the fabrication of the bottom micro electrodes. Figure 4.6 shows the image of the

fabricated wafer with 12 co-planar electrodes. Finally, the Soft Lithography is performed to form the PDMS micro electrodes and bond them to the glass slide.

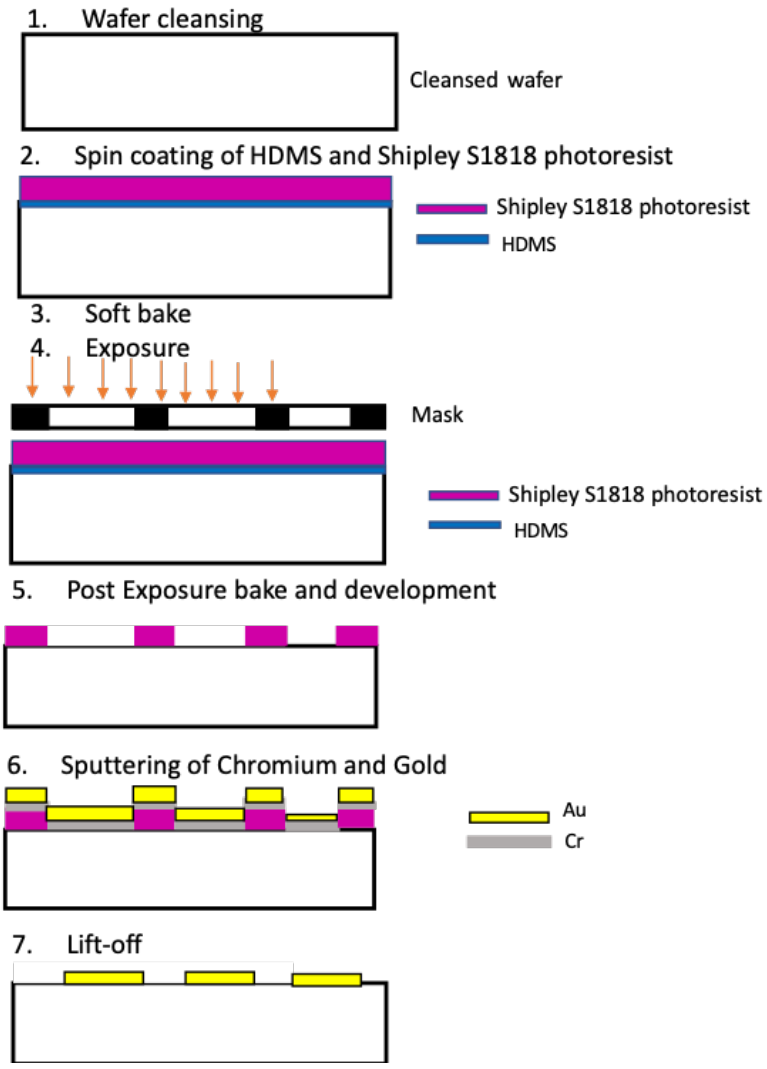

Figure 4.5: Process involved in micro electrode fabrication

4.4 Fabrication of top electrodes

The top electrodes are fabricated by soft lithography. The first step is to develop the SU8 mold on glass wafer by photolithography. PDMS is then poured onto the mold to form the microfluidic channel. Fabrication of microelectrodes involves the following steps. Initially, the PDMS microchannel structure is spin coated with SU-82010 photoresist. The soft

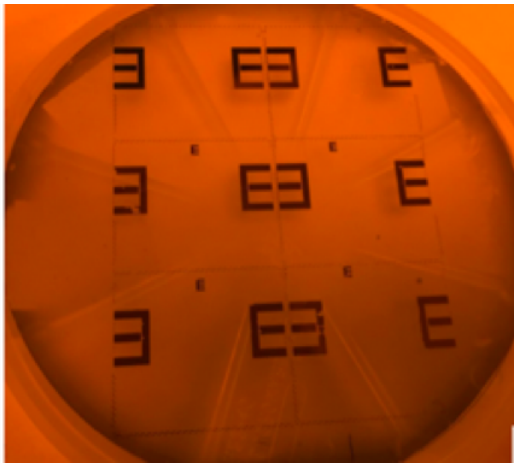

Figure 4.6: Image of fabricated wafer with 12 co-planar electrodes

bake is then performed at $95\ ^{\circ}\mathrm{C}$, followed by the UV Exposure via Chromium mask with exposure energy being 210 mJ/cm^2. The exposed wafer is then developed in SU8 developer for 60 seconds, followed by hard bake at $115\ ^{\circ}\mathrm{C}$ for 150 seconds and cleansing by RF plasma. The patterned PDMS device is then loaded into the sputtering machine and 30 nm of Titanium and 320 nm of Platinum are deposited. Metal coated photoresist is then peeled off from the PDMS surface and the Platinum electrode so obtained is cleansed with acetone, isopropyl alcohol and DI water. For permanent bonding of top and bottom layers, the layers are cleansed with Oxygen RF plasma for 20 seconds prior to bonding, making the PDMS surface hydrophilic.

The layout for the mask design of the top and bottom electrodes was created in Auto-CAD. Figure 4.7 provides the Auto-CAD layout of top and bottom co-planar electrodes.

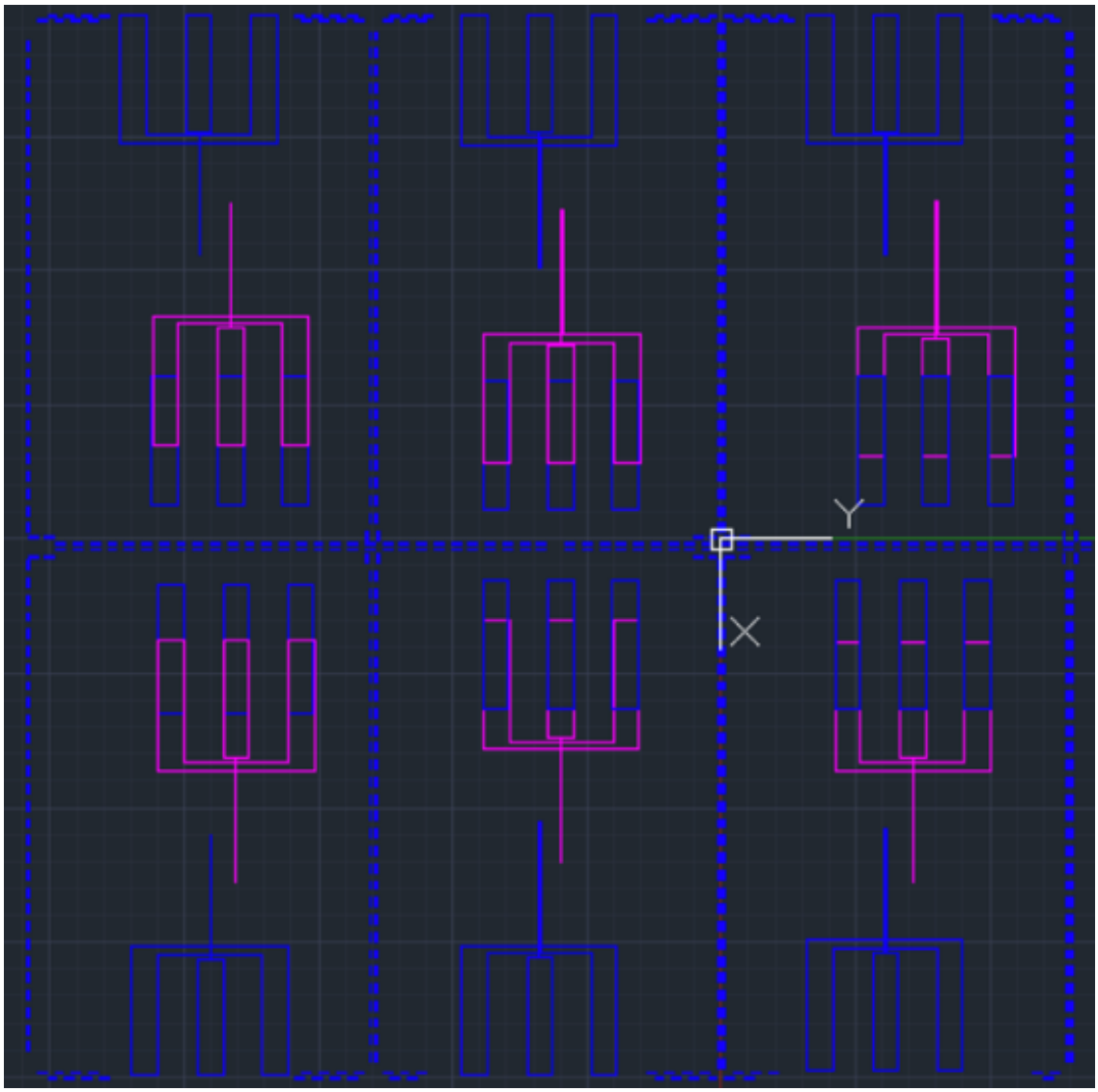

Figure 4.7: Auto CAD layout of top (pink) and bottom (blue) electrode

CHAPTER 5
CONCLUSION AND FUTURE SCOPE

A non fluorescent microfluidic architecture with single excitation and detection scheme using the barcoded particle is proposed in this study. The designed barcoded particle produces distinct electrical signatures when it flows in a microfluidic impedance detection system. The distinct electrical signatures generated by the barcoded particle can perform multiplexing of various biomolecules in an assay. We aim to quantify different proteins expressed by the cell surface using the distinct signatures of the barcoded particle. The proposed microfluidic architecture is sensitive to detect the presence of even a single microsphere conjugated to the barcoded particle. The effect of orientation of microsphere conjugation to the barcoded particle is also investigated. A multi feature selection algorithm is developed to solve the orientation problem and to improve the accuracy of sensing mechanism. The top-bottom microelectrode architecture is proposed for sensitive detection of microspheres conjugated at top and bottom surface of the barcoded particle. The fabrication strategy for the barcoded particle, microfluidic channel and co-planar electrodes is also proposed.

In future, we aim to tag the barcoded particle with antibodies to perform the experiment. We intend to perform the clinical studies for different cell types and explore the effect of magnetization of the conjugated microspheres as they pass over the co-planar electrodes in the channel. The study of disease onset and progression based on cell concentration can also be performed using multiplexed biomarkers.

CHAPTER 6

APPENDIX

6.1 Polydimethylsiloxane (PDMS)

PDMS is a polymer which is employed widely used in the prototyping and fabrication of microfluidic chips from a master mold. The master mold is generated by photolithography can be reused. It is a mineral organic polymer consisting of carbon and silicon group. The PDMS is mixed with the cross-linking agent in the ratio of 10:1 and is then poured over the mold for prototyping. The PDMS surface is inherently hydrophobic and is treated with oxygen plasma and laser treatment to make the surface hydrophilic [26].

The elastomeric polymer has various useful properties like nontoxicity, bio-compatibility, elasticity, transparency and durability. PDMS is bio-inert and hence inhibits the growth of microbes. The bio inertness of PDMS allows it to be used in many biomedical applications. Soft-Lithography is a commonly used fabrication methodology of generating micro architectures using the oxidized PDMS for prototyping.

REFERENCES

[1] Buttarello, Mauro and Plebani, Mario, "Automated blood cell counts: state of the art," *American journal of clinical pathology*, vol. 130, no. 1, 104–116, 2008.

[2] B. Encyclopedia, *Blood-biochemistry*, `https://www.britannica.com/science/blood-biochemistry`, (accessed: 08.17.2019).

[3] M. Brown and C. Wittwer, "Flow cytometry: Principles and clinical applications in hematology," *Clinical chemistry*, vol. 46, no. 8, pp. 1221–1229, 2000.

[4] T. A. Fleisher and J. B. Oliveira, "Flow cytometry," in *Clinical Immunology*, Elsevier, 2019, pp. 1239–1251.

[5] I. ACEA Biosciences, *Novocyte flow cytometer*, `https://www.aceabio.com/products/novocyte-flow-cytometer/`, (accessed: 08.17.2019).

[6] C. Chemistry, *Aacc*, `http://clinchem.aaccjnls.org/`, (accessed: 08.17.2019).

[7] Boorugu, Manish, "Adaptive particle encapsulation using digital opto-fluidic lithography," PhD thesis, Rutgers University-School of Graduate Studies, 2018.

[8] D. R. Rhodes, M. G. Sanda, A. P. Otte, A. M. Chinnaiyan, and M. A. Rubin, "Multiplex biomarker approach for determining risk of prostate-specific antigen-defined recurrence of prostate cancer," *Journal of the National Cancer Institute*, vol. 95, no. 9, pp. 661–668, 2003.

[9] G. MacBeath and S. L. Schreiber, "Printing proteins as microarrays for high-throughput function determination," *Science*, vol. 289, no. 5485, pp. 1760–1763, 2000.

[10] X. Zhao, Y. Zhao, and Z. Gu, "Advances of multiplex and high throughput biomolecular detection technologies based on encoding microparticles," *Science China Chemistry*, vol. 54, no. 8, p. 1185, 2011.

[11] M. Han, X. Gao, J. Z. Su, and S. Nie, "Quantum-dot-tagged microbeads for multiplexed optical coding of biomolecules," *Nature biotechnology*, vol. 19, no. 7, p. 631, 2001.

[12] C.-C. Tsai, K. E. Follis, A. Sabo, T. W. Beck, R. F. Grant, N. Bischofberger, R. E. Benveniste, and R. Black, "Prevention of siv infection in macaques by (r)-9-(2-phosphonylmethoxypropyl) adenine," *Science*, vol. 270, no. 5239, pp. 1197–1199, 1995.

[13] M. Seydack, "Nanoparticle labels in immunosensing using optical detection methods," *Biosensors and bioelectronics*, vol. 20, no. 12, pp. 2454–2469, 2005.

[14] E. F. Petricoin III, A. M. Ardekani, B. A. Hitt, P. J. Levine, V. A. Fusaro, S. M. Steinberg, G. B. Mills, C. Simone, D. A. Fishman, E. C. Kohn, *et al.*, "Use of proteomic patterns in serum to identify ovarian cancer," *The lancet*, vol. 359, no. 9306, pp. 572–577, 2002.

[15] A. L. Washburn, W. W. Shia, K. A. Lenkeit, S.-H. Lee, and R. C. Bailey, "Multiplexed cancer biomarker detection using chip-integrated silicon photonic sensor arrays," *Analyst*, vol. 141, no. 18, pp. 5358–5365, 2016.

[16] R. M. Graybill, M. C. Cardenosa-Rubio, H. Yang, M. D. Johnson, and R. C. Bailey, "Multiplexed microrna expression profiling by combined asymmetric pcr and label-free detection using silicon photonic sensor arrays," *Analytical methods*, vol. 10, no. 14, pp. 1618–1623, 2018.

[17] L. Liotta and E. Petricoin, "Molecular profiling of human cancer," *Nature Reviews Genetics*, vol. 1, no. 1, p. 48, 2000.

[18] C. C. Pritchard, H. H. Cheng, and M. Tewari, "Microrna profiling: Approaches and considerations," *Nature Reviews Genetics*, vol. 13, no. 5, p. 358, 2012.

[19] R. M. Graybill and R. C. Bailey, "Emerging biosensing approaches for microrna analysis," *Analytical chemistry*, vol. 88, no. 1, pp. 431–450, 2015.

[20] A. Gao, X. Yang, J. Tong, L. Zhou, Y. Wang, J. Zhao, H. Mao, and T. Li, "Multiplexed detection of lung cancer biomarkers in patients serum with cmos-compatible silicon nanowire arrays," *Biosensors and Bioelectronics*, vol. 91, pp. 482–488, 2017.

[21] R. Hu, X. Zhang, Q. Xu, D.-Q. Lu, Y.-H. Yang, Q.-Q. Xu, Q. Ruan, L.-T. Mo, and X.-B. Zhang, "A universal aptameric biosensor: Multiplexed detection of small analytes via aggregated perylene-based broad-spectrum quencher," *Biosensors and Bioelectronics*, vol. 92, pp. 40–46, 2017.

[22] P. He, I. Katis, R. Eason, and C. Sones, "Rapid multiplexed detection on lateral-flow devices using a laser direct-write technique," *Biosensors*, vol. 8, no. 4, p. 97, 2018.

[23] C. Li, K. Wen, T. Mi, X. Zhang, H. Zhang, S. Zhang, J. Shen, and Z. Wang, "A universal multi-wavelength fluorescence polarization immunoassay for multiplexed detection of mycotoxins in maize," *Biosensors and Bioelectronics*, vol. 79, pp. 258–265, 2016.

[24] K. C. Cheung, M. Di Berardino, G. Schade-Kampmann, M. Hebeisen, A. Pierzchalski, J. Bocsi, A. Mittag, and A. Tárnok, "Microfluidic impedance-based flow cytometry," *Cytometry Part A*, vol. 77, no. 7, pp. 648–666, 2010.

[25] D. Dendukuri, S. S. Gu, D. C. Pregibon, T. A. Hatton, and P. S. Doyle, "Stop-flow lithography in a microfluidic device," *Lab on a Chip*, vol. 7, no. 7, pp. 818–828, 2007.

[26] M. J. Owen and P. J. Smith, "Plasma treatment of polydimethylsiloxane," *Journal of adhesion science and technology*, vol. 8, no. 10, pp. 1063–1075, 1994.